

Study of mode propagation with 632.8-nm laser in tapered fiber

He Chen (陈 和)¹, Junliang Lu (陆均良)², Chengliang Zhao (赵承良)¹,
Botao Cheng (程波涛)¹, and Xuanhui Lu (陆璇辉)^{1*}

¹Optical Institute, Physics Department, Zhejiang University, Hangzhou 310027, China

²School of Management, Zhejiang University, Hangzhou 310058, China

*E-mail: xhlu@zju.edu.cn

Received December 26, 2008

The material dispersion of a tapered fiber is described by Sellmeier's equation. The dependence of refractive index on wavelength and doping concentration is discussed. A He-Ne laser with the output wavelength of 632.8 nm is used in the experiment. When the cutoff frequency of the fiber is less than the laser frequency, the guiding modes of a single-mode fiber (at 1550 nm) are investigated. The results show that the original single-mode fiber becomes a multi-mode waveguide. The propagation and mode coupling of the light in the taper region are analyzed. By controlling the taper end size of the fiber, the unique tapered fiber can convert a multi-mode beam into a single-mode one.

OCIS codes: 060.2310, 060.2430, 140.3300.

doi: 10.3788/COL20090709.0771.

In recent years, tapered optical fiber has been widely studied and applied in many fields such as biochemical sensor^[1], near-field scanning optical microscope^[2], laser coupling devices^[3,4], and fiber lasers^[5], because it has linear characteristics in evanescent field interaction, mode coupling, mode filtration, and transformation. It also has great potential values in applications for optical coherent photography and frequency measurement since it can form supercontinuum spectrum^[6] due to its big nonlinear coefficient when the size of the fiber is reduced. In this letter, we get image scanning using fiber arrays and the light source of a He-Ne laser, whose wavelength (632.8 nm) is shorter than the cutoff wavelength of the fiber. Under this condition, original single-mode fiber at 1550 nm is turned to multi-mode fiber in that wavelength band, but in practical application single mode operation is desired. Single-mode operation can be obtained by designing and fabricating a tapered fiber properly.

For the tapered fiber that achieves single-mode operation, the mode conversion when the radiating field wavelength is larger than the cutoff wavelength have already been reported^[7-9]. If the tapered fiber is adiabatic^[8], the mode fluctuation caused by the change of fiber size can be considered small enough that the induced power loss in the mode conversion from fundamental mode to high-order modes can be ignored. The conversion process for the light propagation in the tapered fiber can be simply described as follows. At the beginning, light propagates in the fiber core, and most of the energy is concentrated in the core. In the tapered part, the core diameter reduces gradually, and as the refractive index difference between the core and the cladding is so small, the fibers can no more support the mode propagation in the core. Light leaks to the cladding layer and propagates as the radiating mode. We call the point where the propagating mode is turned from core mode to cladding mode as a critical point, or the cutoff point of core mode. For a given tapered fiber, the transmission coefficient V_{cc} from the core mode to the cladding mode can be expressed as^[10] $V_{cc} \approx \sqrt{2/\ln s} (1 + 0.26/\ln s)^{1/2}$, where s is the

ratio of the cladding diameter to the core diameter, independent of wavelength, and is considered invariable in the tapered part. The unitary frequency V at a point z of the fiber core which is related to the wavelength λ can be written as

$$V_{\text{core}}(z) = \frac{2\pi \cdot r_{\text{core}}(z)}{\lambda} \cdot \sqrt{n_{\text{co}}^2 - n_{\text{cl}}^2}, \quad (1)$$

where r_{core} is the core radius, n_{co} and n_{cl} are refractive indices of the fiber core and cladding, respectively. When $V_{\text{core}}(z) > V_{cc}$, light propagates in core mode. At the critical point, $V_{\text{core}}(z) = V_{cc}$. If the local unitary frequency $V_{\text{core}}(z)$ is too small to restrict the core mode, $V_{\text{core}}(z) < V_{cc}$, the cladding will become the new waveguide medium and light will propagate in cladding mode.

If a radiating source whose wavelength is shorter than the fiber's cutoff wavelength is used, Rayleigh scattering will increase and make the propagating loss increase rapidly. On the other hand, the material dispersion induces the change of refractive index of the doped fiber, thus, it redistributes the propagation energy. In the experiment, propagation distance l is very short ($l < 1$ m). In real applications, we only consider the influence of dispersion. Usually, quartz optical fiber is manufactured by doping different materials in SiO_2 to form the core and cladding with a small refractive index difference. The refractive index will increase when GeO_2 or P_2O_5 is doped and decrease when B_2O_3 is doped. Here we consider a special situation that the cladding is pure SiO_2 and the core is SiO_2 with a small amount of GeO_2 dopant. The dependence of the refractive index n on wavelength and doping concentration can be expressed by Sellmeier's equation^[11]

$$n^2 = 1 + \sum_{i=1}^3 \frac{a_i \times \lambda^2}{\lambda^2 - b_i^2}. \quad (2)$$

In Eq. (2), the unit of wavelength λ is micron, and $0.21 \mu\text{m} < \lambda < 3.71 \mu\text{m}$, a_i and b_i ($i = 1, 2, 3$) are related to the materials. According to Refs. [11,12], Table 1 gives the values of a_i and b_i for some materials.

Table 1. Parameters in Sellmeier’s Equation of Pure SiO₂ and GeO₂-Doped Quartz Glass

GeO ₂ Concentration (mol%)	<i>a</i> ₁	<i>a</i> ₂	<i>a</i> ₃	<i>b</i> ₁	<i>b</i> ₂	<i>b</i> ₃
0	0.6961663	0.4079426	0.8974794	0.0684043	0.1162414	9.8961610
3.1	0.7028554	0.4146307	0.8974540	0.0727723	0.1143085	9.8961609
6.3	0.7083925	0.4203993	0.8663412	0.0853842	0.1024839	9.8961750
8.7	0.7133103	0.4250904	0.8631980	0.0831282	0.1079664	9.8961781
11.2	0.7186243	0.4301997	0.8543265	0.0634539	0.1277683	9.8961811
15.0	0.7249180	0.4381220	0.8221368	0.0871572	0.1078145	9.8961973

Via Sellmeier’s equation and the parameters in Table 1, we can get the changes in refractive index according to the GeO₂ concentration at certain wavelength bands. Figure 1 shows the calculated data of refractive index varying with the GeO₂ concentration. It can be easily found that the refractive index has a linear relationship to the doping concentration of GeO₂, and by linear regression we can deduce the linear equation.

If the refractive index is known, the corresponding GeO₂ concentration can be obtained through the linear function. Considering such an optical fiber with the refractive index of cladding *n*_{cl} = 1.444 at λ = 1550 nm and the relative index difference Δ is 0.36%, we know that the GeO₂ doping concentration of the core is 3.68%. For the wavelength of 632.8 nm, the refractive index of the cladding is *n*_{cl} = 1.457. According to the calculated 3.68% doping concentration of the fiber core and the linear relationship, it can be seen that the refractive index of the core is *n*_{co} = 1.46237 and Δ is 0.367%, larger than those at 1550 nm.

In the tapered optical fiber shown in Fig. 2, the optical field propagates along *z*-direction. For a given position *z*, the intensity distribution of optical field is the function of the propagation constant β. Under the weak guidance approximation, the transverse field distribution can be obtained by solving the scale wave equation as^[13]:

$$r^2 \frac{\partial^2 \Psi}{\partial r^2} + r \frac{\partial \Psi}{\partial r} + [r^2 (n^2 k_0^2 - n_{\text{eff}}^2 k_0^2) - m^2] \Psi = 0, \quad (3)$$

where *r* is the distance from the center of fiber to a certain point along the fiber radius, Ψ is the electrical field, *n*_{eff} is the mode efficiency, *m* describes the number of points where the field azimuth angle equals zero and its value is 0 or a positive integer. The fundamental mode is LP₀₁ where *m* = 0. If a mode can be supported in the fiber, *n*_{eff} and the propagation

constant β can be related by β = 2π*n*_{eff}/λ where *n*_{cl} ≤ *n*_{eff} ≤ *n*_{co}. The solution of Eq. (3) is the linear combination of Bessel function and modulated Bessel function. According to the boundary condition, and the wave function and its first order derivative are continuous at the interfaces between fiber core and cladding, cladding and air. Then the propagation constant β of the mode at position *z* can be solved.

Considering the optical field propagation before the fiber is tapered, the intrinsic single-mode propagation will vary because the frequency of the light is higher than the fiber cutoff frequency. For a fiber with the cladding diameter *D* = 125 μm and the core diameter *d* = 8.9 μm, the unitary frequency *V* of optical fiber at 632.8 nm is

$$V = \frac{2\pi}{\lambda} \cdot \frac{d}{2} \cdot \sqrt{n_{\text{co}}^2 - n_{\text{cl}}^2}. \quad (4)$$

By using the datum above, we can get *V* = 5.523, but the single-mode propagation requires *V* < 2.405. So when λ = 632.8 nm, there are five modes supported: LP₀₁, LP₀₂, LP₁₁, LP₂₁, and LP₃₁. In order to get the efficient effective refractive index of each mode, we can numerically solve

Table 2. Propagation Modes and Effective Refractive Indices

Mode	<i>n</i> _{eff}
LP ₀₁	1.4616489
LP ₀₂	1.4587368
LP ₁₁	1.4605596
LP ₂₁	1.4591670
LP ₃₁	1.4575387

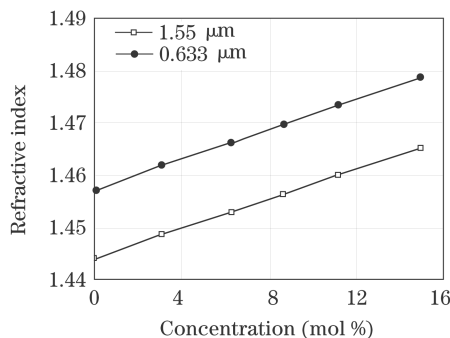


Fig. 1. Variation of refraction index with GeO₂ doping concentration.

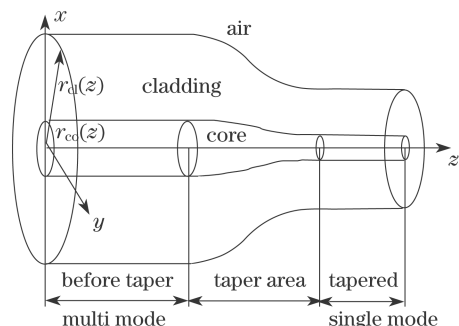


Fig. 2. Sketch of the tapered fiber.

$$\frac{U \cdot J_{j-1}(Ud/2)}{J_j(Ud/2)} = -\frac{W \cdot K_{j-1}(Wd/2)}{K_j(Wd/2)}, \quad (5)$$

where the mode parameters $U = k_0 \sqrt{n_{co}^2 - n_{eff}^2}$ and $W = k_0 \sqrt{n_{eff}^2 - n_{cl}^2}$, $k_0 = 2\pi/\lambda$, $J_j(x)$ and $K_j(x)$ are the j th-order first kind Bessel function and modulated second kind Bessel function, respectively. Table 2 shows the solutions.

In the tapered region, the modes will couple to each other because of the disturbance of field propagation as the gradual reduction of the core diameter. Generally, if we consider that fiber taper is axially symmetrical, mode coupling mainly occurs between the radial modes with the same azimuth symmetry^[8,14]. For example, the fundamental mode LP₀₁ only couples to the high-order mode as LP_{0m}, and the strongest coupling happens with the mode LP₀₂ whose propagation constant is much close to the fundamental mode. Such a situation mostly appears in tapered single-mode fiber. For the tapered multi-mode fiber in this letter, with the decrease of core diameter, a part of the high-order mode energy couples to the radiating mode as the loss, the others couple to lower-order modes. If the fiber taper end size is small enough, the high-order modes are not supported, and the single-mode output can be obtained. Thus, the optical field is still conducted by the interface between cladding and core. The core mode is not cut off yet.

Using the above fiber structure, the ratio of the cladding diameter to the core diameter is $s = D/d = 14$, and the corresponding core-cladding mode transmission coefficient $V_{cc} = 0.83$. When the conversion from core mode to cladding mode happens at the point where the core diameter is $1.335 \mu\text{m}$, the fiber diameter is $18.69 \mu\text{m}$ if s keeps constant in the taper. In order to get single-mode propagation, the unitary frequency must be $V < 2.405$, and then the cladding diameter should be less than $54.166 \mu\text{m}$ and the diameter of fiber core should be no larger than $3.87 \mu\text{m}$ (the visible light single-mode fiber's typical core size is $3\text{--}6 \mu\text{m}$). When the core mode is converted to cladding mode, air acts as the new cladding, the former cladding acts as the fiber core, and the former fiber core's influence can be ignored as the reduction of fiber size. The field will propagate in the fiber in multi-mode form again. So in order to get single-mode output, we should control the end size of the tapered fiber. Moreover, the cladding diameter D' of the output end after taper-pulling should satisfy

$$\frac{2V_{cc} \cdot s}{k_0 \sqrt{n_{co}^2 - n_{cl}^2}} < D' < \frac{4.81s}{k_0 \sqrt{n_{co}^2 - n_{cl}^2}}. \quad (6)$$

The experimental setup for detecting the light mode propagating in the fiber is shown in Fig. 3. An attenuator is used to prevent the saturation of charge-coupled device (CCD). A $20\times$ microscope objective lens and a 0.5-m -long single-mode optical fiber (at 1550 nm) are used. The optical field distribution at the output end of the fiber can be observed with a computer.

It has been discussed that the fiber is a multi-mode fiber for the 632.8-nm light before the taper. Mode coupling will happen by bending the fiber. Different propagation modes will be excited by choosing different positions of the field at the input end or changing the

light incident angle. Besides, during propagation in the fiber, multi-mode diffraction effect exists as modes of different orders have different transmission constants, so that phase differences will exist between each other and then diffraction occurs. Figure 4 shows the simulation results of special optical field propagation in the fiber by using BeamPROP software according to the beam propagation law. We choose Gaussian mode as the launching field whose center displacement to the fiber center is $(2,0)$. When the Gaussian beam's width is a half of the waveguide, there are four modes excited, LP₀₁, LP₀₂, LP₁₁, and LP₃₁. From Fig. 4, we can find that the image of launching field is shown periodically along the propagation direction. Such a self-imaging effect is the basic working principle of multi-mode interference coupling. And this multi-mode interference induces the periodic variation of energy distribution on the fiber cross section along the propagation direction. In a word, in the small port of tapered fiber, the field distribution at the output port varies. It depends on the propagation distance, the position or incidence angle of light at the fiber input port, the bending degree of the fiber, etc. Figure 5 shows some field distribution images taken in the experiment by changing the conditions described above. The field distribution can be converted from one to another.

There are several methods to make tapered fiber, for example, fire extending^[15], chemical etching^[16], CO₂ laser fabrication^[17], etc. In this experiment, the tapered fiber is made by putting a bare fiber on the alcohol lamp flame and pulling it. Figure 6 shows the photograph of the tapered fiber. Its end size is about $45 \mu\text{m}$, and core diameter is $3.6 \mu\text{m}$ which satisfies the single-mode output condition.

We got the smooth tapered fiber by pulling it in the

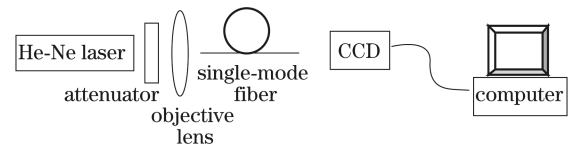


Fig. 3. Experimental setup.

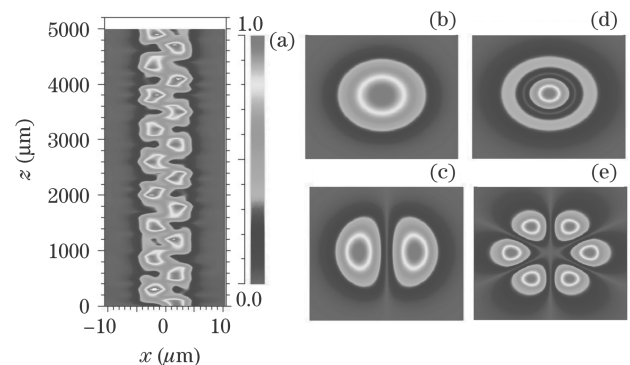


Fig. 4. Propagation and excited modes of Gaussian beam in the small port of tapered fiber. (a) Propagation mode; (b) $m = 0$, $n_{eff} = 1.461649 + 9.801 \times 10^{-11}$; (c) $m = 1$, $n_{eff} = 1.460559 + 7.069 \times 10^{-10}$; (d) $m = 2$, $n_{eff} = 1.458738 + 3.459 \times 10^{-8}$; (e) $m = 3$, $n_{eff} = 1.457539 + 1.829 \times 10^{-7}$.

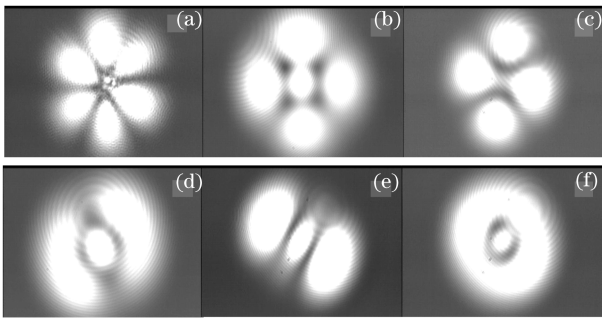


Fig. 5. Output field distributions obtained experimentally in the small port of tapered fiber.

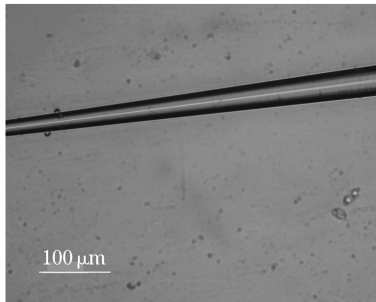


Fig. 6. Tapered fiber.

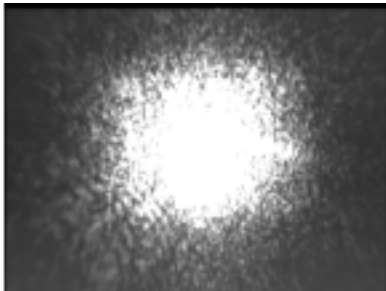


Fig. 7. Field distribution at the output end of tapered fiber.

flame, chose the end, and then cut it carefully to make the size of output end satisfy Eq. (3). The single-mode output of the beam was observed, as shown in Fig. 7. Because the output face is not perfectly flat, a part of the light is diffracted and scattered.

In conclusion, when the wavelength of the light is 632.8 nm which is shorter than the cutoff wavelength of the single-mode fiber, the single-mode fiber becomes a multi-mode fiber. By using Sellmeier's equation to describe the dispersion of the fiber material, we can get the variation for refractive index along with the wavelength under a certain doping concentration. The tapered fiber

can convert the multi-mode beam to a single-mode beam. We analyze the propagation mode of He-Ne laser in the single-mode fiber for 1550 nm whose cutoff frequency is lower than the light frequency and calculate the size of the fiber taper end when the single-mode output can be obtained. The stimulation results agree well with the experiment results.

This work was supported by the Project of Science and Technology of Zhejiang Province, China (No. 2005C21003), the National High Technology Research and Development Program of China (No. 2007AA12Z130), and the State Key Laboratory of Precision Spectroscopy, East China Normal University.

References

1. Z. M. Hale, F. P. Payne, R. S. Marks, C. R. Lowe, and M. M. Levine, *Biosens. Bioelectron.* **11**, 137 (1996).
2. D. W. Pohl and D. Courjon, (eds.) *Near Field Optics* (Kluwer Academic, Boston, 1993).
3. A. Kosterin, V. Temyanko, M. Fallahi, and M. Mansuripur, *Appl. Opt.* **43**, 3893 (2004).
4. Y. Wu, Y. Zheng, S. Li, and J. Wang, *Acta Opt. Sin.* (in Chinese) **27**, 1111 (2007).
5. L. Li, Q. Lou, J. Zhou, J. Dong, Y. Wei, S. Du, and J. Li, *Chin. J. Lasers* (in Chinese) **34**, 1625 (2007).
6. T. A. Birks, W. J. Wadsworth, and P. St. J. Russell, *Opt. Lett.* **25**, 1415 (2000).
7. A. W. Snyder and J. D. Love, *Optical Waveguide Theory* (Chapman and Hall, London, 1983).
8. J. D. Love, W. M. Henry, W. J. Stewart, R. J. Black, S. Lacroix, and F. Gonthier, *IEEE Proceedings J* **138**, 343 (1991).
9. D. Marcuse, *J. Lightwave Technol.* **5**, 125 (1987).
10. R. J. Black and R. Bourbonnais, *IEEE Proceedings J* **133**, 377 (1986).
11. P. S. M. Pires, D. A. Rogers, E. J. Bochove, and R. F. Souza, *IEEE Trans Microwave Theory Tech.* **30**, 131 (1982).
12. T. Izawa and S. Sudo, *Optical Fibers: Materials and Fabrication* (KTK Scientific, Tokyo, 1987).
13. G. Keiser, *Optical Fiber Communications* (3rd edn.) (in Chinese) Y. Li, M. Cui, and T. Pu, (trans.) (Publishing House of Electronics Industry, Beijing, 2000).
14. L. C. Bobb, P. M. Shankar, and H. D. Krumboltz, *J. Lightwave Technol* **8**, 1084 (1990).
15. P. N. Moar, S. T. Huntington, J. Katsifolis, L. W. Cahill, A. Roberts, and K. A. Nugent, *J. Appl. Phys.* **85**, 3395 (1999).
16. Y. Yang, J. Lee, K. Reichard, P. Ruffin, F. Liang, D. Ditto, and S. Yin, *Opt. Commun.* **249**, 129 (2005).
17. T. E. Dimmick, G. Kakarantzas, T. A. Birks, and P. St. J. Russell, *Appl. Opt.* **38**, 6845 (1999).